Title: **Activity-dependent long-term plasticity of afferent synapses on grafted stem/progenitor cell-derived neurons**

Authors: Andreas Toft Sørensen[1], Nina Rogelius[2,3], Cecilia Lundberg[2] and Merab Kokaia[1]*

Author affiliations: [1]Experimental Epilepsy Group, Wallenberg Neuroscience Center, Lund University Hospital, 221 84 Lund, Sweden. [2]CNS Gene Therapy Unit, Wallenberg Neuroscience Center, Department of Experimental Medical Science, Lund University, 221 84 Lund, Sweden. [3]Present address: Genovis AB, Lund, Sweden,

A. Sørensen: andreas.toft_sorensen@med.lu.se

N. Rogelius: nina.rogelius@genovis.com

C. Lundberg: cecilia.lundberg@med.lu.se

M. Kokaia: merab.kokaia@med.lu.se

Corresponding author:

Merab Kokaia, PhD, Prof, Experimental Epilepsy Group, Division of Neurology, Wallenberg Neuroscience Center, BMC A-11, Sölvegatan 17, Lund University Hospital, 221 84 Lund, Sweden.

Tel.: +46 (0)46 2220547

Fax: +46 (0)46 2220560

E-mail: merab.kokaia@med.lu.se

www.med.lu.se/klinvetlund/eeg

Key words: functional integration; long-term potentiation; stem/progenitor cell-derived neurons; synaptic plasticity; transplantation.

ABSTRACT

Stem cell-based cell replacement therapies aiming at restoring injured or diseased brain function ultimately rely on the capability of transplanted cells to promote functional recovery. The mechanisms by which stem cell-based therapies for neurological conditions can lead to functional recovery are uncertain, but structural and functional repair appears to depend on integration of transplanted cell-derived neurons into neuronal circuitries. The nature by which stem/progenitor cell-derived neurons synaptically integrate into neuronal circuitries is largely unexplored. Here we show that transplanted GFP-labeled neuronal progenitor cells into the rat hippocampus exhibit mature neuronal morphology following 4-10 weeks. GFP-positive cells were preferentially integrated into the principal cell layers of hippocampus, particularly CA3. Patch-clamp recordings from GFP-expressing cells revealed that they generated fast action potentials, and their intrinsic membrane properties were overall similar to endogenous host neurons recorded in same areas. As judged by occurrence of spontaneous excitatory postsynaptic currents (EPSCs), transplanted GFP-positive cells were synaptically integrated into the host circuitry. Comparable to host neurons, both paired-pulse depression and facilitation of afferent fiber stimulation-evoked EPSCs were observed in GFP-positive cells. Upon high-frequency stimulation, GFP-positive cells displayed post-tetanic potentiation of EPSCs, in some cases followed by long-term potentiation (LTP) lasting for more than 30 min. Our data show for the first time that transplanted neuronal progenitor cells can become functional neurons and their afferent synapses are capable of expressing activity-dependent short and long-term plasticity. These synaptic properties may

facilitate host-to-graft interactions and regulate activity of the grafted cells promoting functional recovery of the diseased brain.

INTRODUCTION

Recent progress in research of experimental cell-replacement therapies has provided evidence that various neural stem cells might become a potential source for transplantation in human neurological disorders (Gage, 2000; Kim and de Vellis, 2009; Lindvall and Kokaia, 2006). In Parkinson's disease, stroke, Alzheimer's disease, and epilepsy degeneration of certain population of neurons is believed to play a critical pathogenic role (Glass and Dragunow, 1995; Kish et al., 1988; Whitehouse et al., 1981). Although the severity of these disorders varies, these conditions are often intractable and major clinical symptoms persist despite extensive treatment with available drugs.

Multipotent neural stem cells are characterized by their ability of self-renewal and potential of giving rise to highly purified progenitor cells. In animal models, transplanted neural stem cell-derived progeny can incorporate into the brain parenchyma, giving rise to both neuronal and glial lineages (Conti et al., 2008; Gottlieb, 2002). Partial reconstruction of damaged neuronal circuitries yielding functional improvement has also been demonstrated in various animal models, such as multiple sclerosis, Huntington's disease and Parkinson's disease (Armstrong et al., 2002; Glaser et al., 2005; Madhavan et al., 2009; McBride et al., 2004). Enhanced functional recovery could potentially also be achieved by combining cell replacement with *ex vivo* gene transfer, whereby genetically modified neural stem cell-derived progeny could release therapeutically active compounds after grafting (Behrstock and Svendsen, 2004; Li et al., 2007; Martinez-Serrano and Bjorklund, 1997).

The ability of transplanted neural stem cell-derived neurons to establish functional synaptic connections with existing host neurons and integrate into neuronal circuitries is believed to be a prerequisite for functional recovery (Lindvall and Kokaia, 2010; Rosser et al., 2007; Shetty and Hattiangady, 2007). Several steps are required to accomplish such integration, including cell migration, differentiation, synaptic target selection and development of both axonal and dendritic compartments capable of receiving and transferring synaptic information. Such integration of transplanted cells is most probably guided by local environmental cues including signaling molecules and host neuronal circuit activity sensed by their afferent synapses. Therefore, plasticity of their afferent synapses in response to activity of surrounding host neurons may prove crucial for the integrative capacity of these cells. We and others have previously shown, that immortalized and genetically GFP-labeled neural progenitor cells after transplantation into the cortex or hippocampus of neonatal and adult rats can undergo region-specific differentiation yielding numerous GFP-labeled neurons (Englund et al., 2002; Englund et al., 2000; Lepski et al., 2010; Lundberg et al., 2002; Shihabuddin et al., 1995; Shihabuddin et al., 1996). When fully differentiated, these cells preferentially display morphological features of endogenous neurons, particularly pyramidal cells. They can establish cortico-thalamic and contra-lateral hippocampal axonal connections after transplantation into the cortex or hippocampus, respectively, mimicking already existing normal anatomical connections of intrinsic neurons. Integration into the brain is not only limited to neural stem/progenitor cell derived-neurons from rodents, but can also take place for fetal neuronal precursor cells derived from humans (Maciaczyk et al., 2009). Electrophysiological evidences have shown that rodent stem cell-derived neurons after transplantation can display properties of functional neurons and become

synaptically integrated into neuronal circuitries. Formation of excitatory synapses with AMPA and N-methyl-D-aspartate (NMDA)-type glutamate receptors and inhibitory GABAergic synapses have been described (Auerbach et al., 2000; Benninger et al., 2003; Englund et al., 2002; Ruschenschmidt et al., 2005; Wernig et al., 2004). Such excitatory afferent connections can display pronounced paired-pulse facilitation (PPF) indicative of normal presynaptic short-term synaptic plasticity in newly established synapses (Benninger et al., 2003; Englund et al., 2002; Ruschenschmidt et al., 2005; Wernig et al., 2004). In the present study, we now further characterize the functional properties of GFP-labeled neural progenitor-derived neurons after transplantation into hippocampus **of neonatal rats**, and demonstrate for the first time ability of their host-derived afferent excitatory synapses to display activity-dependent long-term potentiation (LTP). This type of long-term synaptic plasticity is considered an essential feature of excitatory cortical synapses, important for developmental maturation of connectivity and formation of new memories (Cooke and Bliss, 2006; Lynch, 2004).

MATERIALS AND METHODS

Cell culture and lenti-viral transduction. The condition and preparation of the cell line has been described in detail elsewhere (Lundberg et al., 2002; Whittemore and White, 1993). Briefly, the conditionally immortalized neural progenitor cell line, RN33B, derived from rat embryonic Sprague-Dawley (SD) raphe nuclei, was generated by retroviral transduction of the temperature-sensitive simian virus 40 large-T-antigen and expanded. The cell line was grown at its permissive temperature at 33°C in polyornitine-coated flasks in medium consisting of DMEM/F12, 1% penicillin/streptomycin, 1% glucose, 1.5% $NaCO_3$ and 10% FBS. A

recombinant lenti-viral vector carrying the reporter gene for enhanced GFP (Rosenqvist et al., 2002) was added to the culture medium (multiplicity rate of 5, based on the transducing units/ml on 293T cells) for 48 hours, after which the medium was changed. After transduction, approximately 85% of the cells expressed GFP. Subsequently, cells were sorted as single cells for autofluorescent using FACS, defined as the fraction of cells with fluorescence between 300 and 10.000 arbitrary fluorescence units, resulting in a near 100% GFP-positive population. Cells were trypsinated with density of 100.000 cells per µl in HBBS before transplantation.

Transplantation. For transplantation, 72 neonatal rats derived from time-mated female SD rats (B&K Universal, Stockholm, Sweden) were used as recipients. Rats were weaned approximately three weeks after birth and kept in 12-hours light/dark cycles with free access to laboratory food and water. All experimental procedures were approved and carried out according to rules set by the local Ethical Committee following the European Community Council Directive for the Care and Use of Laboratory Animals. On postnatal days 1-2 (P1-2), rats were anesthetized by hypothermia and placed into a stereotaxic frame. A 2-µl Hamilton syringe fitted with a thin glass pipette was used to bilaterally inject 1 µl cell suspension (0.1 µl/min) at each injection site (in mm): anteroposterior (AP): -1.2, mediolateral (ML): ±1.5, dorsoventral (DV): -1.5 into the intact brain. The AP and ML, and DV coordinates were calculated from bregma and dura surface, respectively (Paxinos and Watson, 1996). The injection pipette was left in place for an additional 5 min to minimize backflow of injected cells.

Brain slices. Four to ten weeks after cell transplantation, rats were killed by decapitation and after rapid removal of their brain, the hippocampi were dissected in ice-cold and oxygenated (95% O_2 and 5% CO_2) sucrose solution containing (in mM): sucrose 195, KCl 2.5, $CaCl_2$ 0.5, $MgCl_2$ 7, $NaHCO_3$ 28, NaH_2PO_4 1.25, glucose 7, ascorbate 1, pyruvate 3 (pH 7.4 and mOsm 300). In the same solution, transverse slices of 210 or 350 μm thickness were cut on a vibratome (Vibratome 3000, Ted Pella, Inc., Redding, CA) and stored at room temperature (RT) in a chamber containing oxygenated artificial cerebrospinal fluid (aCSF) consisting of (mM): NaCl 119, KCl 2.5, $MgSO_4$ 1.3, $CaCl_2$ 2.5, $NaHCO_3$ 26.2, NaH_2PO_4 1, glucose 11 (pH 7.4 and 295 mOsm). After more than 1 hour of resting, individual slices were transferred to a submerged recording chamber continuously perfused with oxygenated aCSF at 2-3 ml per min at RT. GFP-labeled cells were visualized using a wide-band excitation filter (450-480 nm), whereas visual approach for whole-cell patch-clamp was performed under infrared differential interference contrast (IR-DIC) guidance. GFP-labeled cells appearing viable and fully differentiated with cell soma within the principal cell layers of the hippocampus, i.e. stratum granulosum of the dentate gyrus, or stratum pyramidale of CA1 or CA3 were selected for recordings. Endogenous host principal cells were recorded from identical areas.

Whole-cell patch-clamp electrophysiology. Patch pipettes were pulled from heat-sterilized borosilicate glass capillaries and filled with: for current-clamp recordings of intrinsic membrane properties (mM): K-gluconate 122.5, KCl 17.5, NaCl 8, KOH-HEPES 10, KOH-EGTA 0.2, MgATP 2, and Na_3GTP 0.3; for voltage-clamp recordings of synaptic inputs (mM): K-gluconate 117.5, CsCl 17.5, NaCl 8, CsOH-HEPES 10, CsOH-EGTA 0.2, MgATP 2, Na_3GTP 0.3, and QX-314 5. Pipette

solutions were adjusted to pH 7.2 and osmolarity of 295 mOsm, and biocytin (0.5-1 mg/ml) was added immediately before use, all resulting in pipette resistances of 4-6 MΩ. HEKA amplifier and software (EPC-9 and PATCHMASTER, HEKA Elektronik, Lambrecht/Pfalz, Germany) were used for data acquisition. The junction potential was automatically corrected by the amplifier software, and data were continuously filtered at 2.9 kHz and sampled at 10 kHz. Off-line analysis was performed using FITMASTER (HEKA Elektronik) and Igor Pro (WaveMetrics, Lake Oswego, USA) software. All results are presented as mean ± SEM and evaluated by Student's t-test, unless otherwise stated. Level of statistical significance was $p < 0.05$.

Resting membrane potential (RMP) was obtained in current-clamp mode immediately after breaking into whole-cell configuration. The recording was continued, if RMP was more negative than –50 mV, and series resistance (not routinely compensated) was within 12-25 MΩ. Test pulses of -5 mV continuously measured access resistance, and recordings were discarded if access resistance varied over time more than 20%. Voltage-dependent rectification (*I-V* relationships) was recorded in current-clamp mode by applying steps of negative and positive current pulses of 500 ms duration at various strengths. Action potential characteristics were analyzed as previously (Jakubs et al., 2006). Briefly, threshold, amplitude (threshold to peak) and duration (at half-amplitude) were measured from the first evoked action potential (as shown in Fig. 2C) induced by step depolarization current pulses of 500 ms duration.

Spontaneous excitatory postsynaptic currents (sEPSCs) were recorded at -70 mV from cells located in CA3 stratum pyramidale. Synaptic events were detected off-line by MiniAnalysis software (Synaptosoft Inc., Decatur, GA) with amplitude of five times or more of average RMS noise level (1.22 ± 0.14 pA, n = 10). Between groups

interevent intervals (IEIs), amplitudes, rise and decay times of the first 100 automatically identified sEPSCs from each cell were compared using the Kolmogorov-Smirnov (K-S) test.

Evoked EPSCs were generated by paired-pulse stimulations with interstimulus interval (ISI) of 100 ms. These stimuli were delivered at 0.067 Hz using a bipolar stainless steel electrode, and the intensity was carefully adjusted to induce submaximal synaptic responses in recorded cells. Average amplitude of 24 consecutive evoked EPSCs was used to determine the paired-pulse ratio, calculated as EPSC[2] divided by EPSC[1]. In some cases, PTX (100 μM; Tocris Cookson Ltd., Avonmouth, UK) was added to the perfusion solution to block $GABA_A$ receptor-mediated transmission. For cells situated in stratum pyramidal of CA3, the electrode was placed in CA3 stratum radiatum for stimulating associational/commissural (A/C) fibers. Since evoked EPSCs in CA3 cells were totally unaffected by DCG-IV application (3 ⌈M; Tocris Cookson), a group II metabotropic glutamate receptor agonist which specifically blocks glutamatergic transmission in mossy fiber-CA3 synapses, these responses were considered as originating from A/C fibers (Kanter-Schlifke et al., 2007; Kirschstein et al., 2004). For cells situated in stratum granulosum of the dentate gyrus or CA1 stratum pyramidale, fibers of the medial perforant path (MPP) or Schaffer collaterals, respectively, were stimulated.

High-frequency stimulation (HFS), delivered at 100 Hz for 1 sec using submaximal stimulations intensities, was used for LTP induction. HFS was applied within 8 min after obtaining the whole-cell configuration, and obtained in current-clamp mode before switching back to voltage-clamp. LTP was considered significant if the mean EPSCs amplitude, as calculated 10–15 min after HFS, was increased by >15% from average baseline values. The induction rate of LTP was compared

between groups using χ^2-test followed by Fisher's exact test. Level of post-tetanic potentiation (PTP) was determined each min (average of four EPSCs per min) during the first 5 min following HFS in each cells, and expressed as a relative change to baseline values.

Immunohistochemistry. Gradual maturation of transplanted GFP-positive cells were determined on day 2, 7, 21 or 28 after transplantation in 8 rats not used for electrophysiology. These rats were deeply anesthetized with pentobarbital and perfused through the ascending aorta with 0.9% NaCl followed by 4% paraformaldehyde. Brains were post-fixed overnight (at 4° C), transferred to 20% sucrose and dehydrated overnight. Brains were cut on a freezing microtome (30 µm thick slices) and free-floating sections were rinsed in KPBS and incubated overnight at RT in 1:10.000 dilution of rabbit anti-GFP (Abcam, Cambridge, UK) in 5% NDS. Slices were rinsed and incubated with 1:200 dilution of secondary FITC-donkey-anti-rabbit (Jackson ImmunoResearch Europe Ltd, Suffolk, UK) in 2% NDS for two hours before mounting on gelatin-coated slides and coverslipped using PVA-DABCO mounting medium. For additional NeuN staining, some slices were incubated in 2% NGS with 1:100 mouse-anti-NeuN (Chemicon, CA, USA) followed by 1:200 Cy3-donkey-anti-mouse (Vector Laboratories, CA, USA). Slices used for electrophysiology were post-fixed overnight in 4% PFA, and rinsed in KPBS. These slices were stained (for GFP visualization) as described above, and with additional application of 1:200 dilution of CyTM3-steptavidin (Jackson ImmunoResearch) for biocytin identification of recorded cells. Epifluorescent or confocal laser-scanning (Leica TCS) microscopy was used for digital imaging.

RESULTS

Progressive maturation of transplanted neuronal progenitor cells. During the first month following transplantation, maturation pattern and fate of GFP-positive neuronal progenitor cells were evaluated by immunohistochemistry at four different time points. On the second day following transplantation, clusters of GFP-positive cells close to the injection site were detected. These cells had either round or elongated cell bodies without displaying dendritic processes (Fig. 1A). After 7 days, some GFP-positive cells had migrated away from the cell clusters at the graft site. These cells were more disperse, and some of them had minor processes (Fig. 1B). After 21 days, a fraction of surviving GFP-positive cells started appearing in the principle cell layers of the hippocampus, particularly in CA3 stratum pyramidale. These cells had small dendritic processes, which began to extend from the cell soma (Fig. 1C). From 28 days and onwards, few GFP-positive cells appeared fully differentiated with multiple branching dendrites resembling normal neurons. These cells were located in the principal cell layers of the hippocampus, oriented perpendicular to the cell layer as host principal cells (Figs. 1D, E and F). From this time point and until 10 weeks after transplantation, whole-cell patch-clamp recordings were attempted in slices from 64 animals. A total of 41 recordings were successfully obtained from GFP-positive cells displaying fully differentiated morphology. Thirty-two cells were recorded in CA3 stratum pyramidale, 4 in CA1 stratum pyramidale and 5 in stratum granulosum of the dentate gyrus. At the time of recordings, the age of transplanted GFP-positive (calculated from day of cell transplantation) and host cells (age of animal) were almost similar; 43.2 ± 0.6 days (range: 26-68) and 47.7 ± 0.3 days (range: 27-68), respectively. Although not further quantified, but in line with

previous observations (Englund et al., 2002; Lundberg et al., 2002), few GFP-positive astrocyte-like cells were also detected in some slices, while round cells with undifferentiated morphology gradually disappeared over time. In most cases, such round cells were undetectable in slices used for electrophysiology 8-10 weeks following transplantation.

Fully differentiated neuronal progenitor cells in CA3 display intrinsic membrane properties similar to host CA3 pyramidal neurons. In CA3, all recorded GFP-positive and host pyramidal cells were capable of generating fast action potentials in response to current injection-induced depolarization (Figs. 2A, B, C and D). The recordings also revealed that RMP, input resistance (R*i*) and membrane voltage rectification were similar between the groups (Table 1, Figs. 2E and F). In contrast, the action potential threshold was significantly higher in GFP-positive (-36.7 ± 1.7 mV) as compared to endogenous CA3 pyramidal cells (-45.2 ± 1.4 mV; $p < 0.01$), while action potential duration and amplitude were equal between groups (Table 1). Generation of spontaneous action potentials was never observed in any of the recorded cells. All recorded cells were retrospectively processed for immunohistochemistry. Staining revealed clear co-labeling of GFP and biocytin in GFP-positive cells (Fig. 2G), and based on the biocytin-labeling of their dendrites, the multiple branching morphology was comparable to the branching of endogenous biocytin-labeled CA3 pyramidal cells (Fig. 2H).

Functional synapses on transplanted neuronal progenitor cell-derived neurons display short-term synaptic plasticity. We next sought to determine whether functional synapses were established between host and transplanted GFP-positive

cells. In CA3 region, sEPSC were recorded from both host and transplanted cells (Fig. 3A). In all GFP-positive cells sEPSCs were recorded. Further analysis revealed significantly shorter IEIs of sEPSCs in GFP-positive cells (241 ± 18 ms; n = 5 cells, $p < 0.001$) as compared to host CA3 pyramidal cells (754 ± 59 ms; n = 5 cells; Fig. 3B). In addition, the amplitudes of sEPSCs were significantly higher (13.4 ± 0.4 pA, $p < 0.01$) in GFP-positive cell as compared to host pyramidal cells (11.2 ± 0.4 pA, Fig. 3C), thus indicating stronger excitatory drive onto transplanted cells. Rise and decay times of sEPSCs were similar between the groups (data not shown).

Next we explored whether excitatory synapses formed on fully differentiated GFP-positive cells in CA3 displayed short-term synaptic plasticity. Paired-pulse stimulations applied to stratum radiatum in the CA3 subfield generated evoked EPSCs that displayed paired-pulse depression (PPD) of equal magnitude in GFP-positive (82 ± 13%; EPSC[1]: 112 ± 19 pA, EPSC[2], 80 ± 14 pA, n = 14 cells) and host CA3 pyramidal cells (83 ± 10%; EPSC[1]: 108 ± 26 pA, EPSC[2]: 81 ± 21 pA, n = 9 cells; Fig. 3D). Application of PTX to the perfusion solution for blocking $GABA_A$ receptors converted PPD of EPSCs into paired-pulse facilitation (PPF) (Fig. 3E), suggesting that $GABA_A$ receptor-mediated inhibition was responsible for observed PPD of evoked EPSCs. The level of PPF in GFP-positive cells (135 ± 8%, n = 14 cells) after PTX application was similar to that in host pyramidal cells (135 ± 5%, n = 6 cells). Retrospective visualization of biocytin-labeled GFP-positive cells and host pyramidal cells in CA3 showed that GFP-positive cells developed dendritic spines that were of similar appearance as those on host neurons (Figs. 3F and G), thus supporting the electrophysiological evidences of functional synapse formation on transplanted GFP-positive cells.

Due to more infrequent incorporation of fully differentiated GFP-positive cells into CA1 stratum pyramidale and stratum granulosum of the DG, only few successful recordings of such cells were obtained. Nevertheless, these recordings support the notion that formation of functional synapses is not unique for grafted GFP-positive cells situated in CA3 stratum pyramidale only. This is also the case for fully differentiated neuronal progenitor cells in DG and CA1 with neuronal phenotype (Suppl. figs. 1A, B, C and D). It also appears that GFP-positive cells in these regions can adopt intrinsic membrane properties similar of endogenous CA1 pyramidal and granule cells, respectively (see more details in supplementary data).

Activity-dependent LTP in afferent synapses of grafted GFP-positive cells. One prominent feature of the hippocampus is its involvement in cognitive function, wherein long-term plasticity in hippocampal excitatory synapses is considered as an underlying mechanism of learning and memory (Cooke and Bliss, 2006; Lynch, 2004). To our knowledge, it has not been shown previously whether newly formed excitatory synapses onto grafted neuronal stem/progenitor cell-derived neurons can express activity-dependent long-term synaptic plasticity. To address this question, we applied HFS to stratum radiatum in CA3 while recording from transplanted GFP-positive cells located in CA3 stratum pyramidale. In 3 out of 9 recorded GFP-positive cells showing PTP upon HFS, stable LTP of evoked EPSCs lasting for the entire recording period (at least 30 min) was observed (Fig. 4A). The magnitude of LTP appeared comparable to that in host CA3 pyramidal cells. In case of host neurons, PTP was followed by stable LTP in 4 out of 12 cells (Fig. 4A). Thus, induction and expression of LTP in grafted GFP-positive and host CA3 pyramidal cells appeared similar (χ^2-test followed by Fisher's exact test). Also the levels of PTP, a form of

presynaptic short-term plasticity, lasting the first 5 min after HFS, did not differ between the groups (Fig. 4B). In few recordings (4 grafted GFP-positive and 2 host pyramidal cells) PTP was not observed when HFS was applied to afferent axons. All together, these data demonstrate for the first time, that afferent excitatory synapses on transplanted neuronal progenitor cell-derived neurons located in CA3 can express long-lasting synaptic plasticity equivalent to that in host principal neurons. Since application of type 2 metabotropic glutamate receptor group agonist DCG-IV, which presynaptically and selectively suppresses glutamate release from mossy fibers, did not change the EPSC amplitudes (data not shown), LTP was most likely induced in synapses of A/C fibers, as expected also by the positioning of the stimulating electrode.

DISCUSSION

A prerequisite of transplanted neural stem/progenitor cell-derived neurons with neuroregenerative potential is thought to be their ability to integrate functionally into neuronal circuitries. Achieving functional integration together with long-lasting graft survival appears to be of outmost importance in restoring brain function, including memory disturbances (Lindvall and Kokaia, 2010; Miller, 2006). Ideally, surviving transplanted cells should mature into functional neurons, display appropriate membrane properties and be capable of establishing proper synaptic connections with host neurons to participate in network information processing.

In the present study, we show that progeny of an immortalized GFP-labeled neuronal progenitor cell line gradually differentiates into the neuronal lineage after transplantation into the rat hippocampus. On four different time points following transplantation, we carefully traced the fate of transplanted GFP-labeled cells using

immunohistochemistry. In agreement with other studies exploring the same neuronal progenitor cell line as used here, only a minor fraction of transplanted cells survived, and progressively acquired a morphological phenotype associated with the neuronal lineage during the first month following transplantation (Englund et al., 2002; Lundberg et al., 2002; Lundberg et al., 1996; Onifer et al., 1993; Shihabuddin et al., 1995; Shihabuddin et al., 1996). After one month, GFP-positive cells with mature morphological appearance were mainly situated within the principal cell layers, particularly CA3, displaying comparable dendritic morphology as endogenous principal neurons, consistent with previous observations (Englund et al., 2002; Lundberg et al., 2002; Onifer et al., 1993; Shihabuddin et al., 1995).

The gradual migration and development of complex dendritic arbors suggests that transplanted GFP-positive cells requires approximately four weeks to acquire a mature phenotype. What determines the high degree of neuronal specificity in terms of their region-specific morphological appearance is unknown, but cues provided by the local microenvironment seems to be a likely explanation. Preservation of the host tissue environment is also, at least to some extent, necessary for their integration. Complete depletion of host neurons in hippocampal cell layers disorientated the transplanted cells and they acquired multiple processes with no structural polarity (Shihabuddin et al., 1996). Likewise, a GFP-labeled neuronal progenitor cell line derived from the mouse developing hippocampus transplanted into the kainate-lesioned rat hippocampus resulted in a graft comprising all three neural cell lineages. However, probably due to substantial neuronal damage and reactive glial cells, migration and full maturation of neurons was incomplete (Shetty et al., 2008). Thus, preconditioning of the recipient tissue and local neuronal network appears to be important for successful differentiation and integration of such transplanted cells. This

does not however necessarily diminish the importance of using neural stem cells for cell replacement strategies. For example, in chronically epileptic pilocarpin-treated rats with extensive but not complete degeneration of host hippocampal neurons, intrahippocampal transplantation of stem cell-derived neuronal progenitors was shown to give rise to mature and functional neurons, which received synaptic inputs from the host brain (Ruschenschmidt et al., 2005). In this context, usage of neural stem cells for restorative strategies appears to be more promising for partially damaged brain tissue, while more severely degenerated brain tissue may not provide an optimal environment for their regenerative capacity.

Our electrophysiological recordings demonstrated that transplanted GFP-labeled cells not only had morphological profiles of mature neurons but also exhibited functional neuronal properties with normal membrane characteristics, and with ability to generate fast action potentials. The intrinsic membrane properties were identical to those recorded in host CA3 pyramidal cells, except the action potential threshold, which was significantly higher in grafted GFP-positive cells. Thus, stronger membrane depolarization was required to generate action potentials in transplanted cells in CA3 region. Despite few recordings obtained in other regions (supplementary data), it appears that grafted GFP-positive cells migrating and incorporating into CA1 and DG region adopt properties very similar to those of endogenous principal neurons in same locations. In summary, the electrophysiological recordings obtained from grafted GFP-positive cells support the morphological evidence of functional maturation and are in line with the notion of their region-specific integration.

Functional synaptic integration into the host neuronal circuitry was first demonstrated by recordings of sEPSCs in GFP-positive cells situated in CA3 stratum pyramidale. Interestingly, besides revealing that GFP-positive cells receive afferent

synaptic inputs from the host circuitry, analysis of sEPSC frequencies and amplitudes revealed a significantly stronger excitatory drive onto transplanted cells as compared to similarly positioned host CA3 pyramidal cells.

Why the transplanted cells receive stronger glutamatergic drive (both at pre- and postsynaptic sites) is unclear. This may be a compensatory mechanism to balance increased threshold for action potential generation**.** A speculative explanation could be a differential effect exerted by endogenous neurotrophic factors, such as the BDNF, on mature (endogenous) pyramidal and immature (transplanted) cells. BDNF is known to regulate, at least partly, the cell-wide homeostatic plasticity of excitatory synapses. Miniature EPSCs are action potential-independent EPSCs and constitute a fraction of the registered sEPSC obtained in our experimental conditions. Studies have shown that in mature neocortical pyramidal neurons BDNF decreases the amplitude of mEPSCs (Rutherford et al., 1998), while in immature hippocampal neurons it increases frequency of mEPSCs (Collin et al., 2001; Vicario-Abejon et al., 1998). Similar BDNF-induced plasticity of mEPSCs has also been demonstrated in co-culture system of embryonic stem cell-derived neurons in neocortical explants (Copi et al., 2005). Therefore, the increased excitatory synaptic drive onto transplanted cells, as observed in the present study, might represent a BDNF-mediated regulation of homeostatic plasticity affecting transplanted and host neurons differentially. Another possibility is that graft-to-graft synapses may have contributed to the observed increase in excitatory drive onto the grafted cells. However, since very few GFP-labeled cells (usually 1-4 mature cells) were detected in each slice preparation used for recordings, this explanation seems less likely.

To further investigate the synaptic integration of transplanted cells, afferent fibers impinging onto GFP-positive cells were stimulated electrically. Without

blocking $GABA_A$ receptors, paired stimulations of stratum radiatum in CA3 gave rise to PPD of EPSCs of similar ratio in both transplanted and host neurons, suggesting normal short-term synaptic plasticity in afferent synapses of fully differentiated GFP-positive cells. This was further supported by applying PTX to the perfusion solution, which converted PPD into PPF of EPSCs, again with similar ratio between the groups. This indirectly demonstrates that fully mature GFP-positive cells, in addition to glutamatergic receptors, are also expressing functional $GABA_A$ receptors and are receiving functional inhibitory synapses from surroundings interneurons. In neocortex, we have previously provided direct evidence of existence of afferent GABAergic synapses onto transplanted embryonic progenitor-derived GFP-labeled neurons. In this case, evoked inhibitory postsynaptic currents (IPSCs) could be totally blocked by PTX application (Englund et al., 2002). In support, other synaptically connected embryonic stem cell-derived neurons, as investigated in both *in vitro* and *in vivo* conditions, also are capable of receiving inhibitory and excitatory synaptic inputs from the host circuitry (Benninger et al., 2003; Lepski et al., 2010; Ruschenschmidt et al., 2005; Wernig et al., 2004). Whether functional synaptic integration of neuronal stem/progenitor cells occurs similarly after transplantation into the adult brain as compared to the neonatal brain is currently unknown. In previous study, however, the RN33B cell line displayed mature neuronal morphology after transplantation into the adult rat brain (Englund et al., 2000). In accordance, the same cell line can survive and differentiate into functional neuronal phenotype after transplantation into adult rat hippocampus exposed to electrical stimulation-induced status epilepticus (unpublished observations). Thus, cues provided by the local microenvironment, rendering transplanted neuronal stem/progenitor cells to integrate functionally into the

pre-existing network, appears to be present both during brain development, as well as during pathological conditions in adults.

Here we show that grafted GFP-positive cells in CA3 area can display long-term synaptic plasticity for more than 30 min after HFS stimulation of A/C fibers. This provides for the first time evidence that fully differentiated neural stem/progenitor cell-derived neurons are capable of expressing LTP. LTP at synapses of A/C fibers onto CA3 pyramidal neurons requires NMDA receptor activation at postsynaptic site induced by depolarization, and consequent postsynaptic Ca^{2+} influx (Harris and Cotman, 1986; Zalutsky and Nicoll, 1990), which at the end leads to up-regulation of postsynaptic AMPA receptors. Capacity for up-regulation of postsynaptic AMPA receptors, although in more cell-wide manner that is more characteristic for homeostatic plasticity, has been demonstrated in embryonic stem/progenitor cell-derived neurons co-cultured with cortical explants (Copi et al., 2005; Turrigiano, 1999; Turrigiano, 2007; Wierenga et al., 2005). Therefore, it seems feasible that also after HFS, AMPA receptors are upregulated to express LTP. Thus, our results provide proof of principal that transplanted embryonic stem/progenitor cell-derived neurons are capable of participating in the formation of new memories in the hippocampus. This is of particular interest, since neurological disorders that are accompanied by cell loss in the hippocampus, e.g. in patients with severe mesial temporal lobe epilepsy, often are associated with disturbances in learning and memory. Therefore, one could envisage that neural stem cell therapy may also contribute to functional recovery of learning and memory dysfunctions in these patients.

Supplementary materials related to this article can be found online at doi:10.1016/j.expneurol.2011.02.008

DISCLOSURE STATEMENT

The authors indicate no potential conflicts of interest.

ACKNOWLEDGEMENTS: This work was supported by grants from the Swedish Research Council, The Royal Physiographic Society in Lund, Lars Hierta Memorial, Segerfalk, Crafoord and Kock Foundations, and EU Commission FP6 grant EPICURE. ATS was supported by Lundbeck foundation. We thank Prof. Olle Lindvall for comments on the manuscript, and thank Anneli Josefsson for excellent technical support.

REFERENCES

1. Armstrong, R. J., Hurelbrink, C. B., Tyers, P., Ratcliffe, E. L., Richards, A., Dunnett, S. B., Rosser, A. E., and Barker, R. A., 2002. The potential for circuit reconstruction by expanded neural precursor cells explored through porcine xenografts in a rat model of Parkinson's disease. Exp Neurol 175**,** 98-111.

2. Auerbach, J. M., Eiden, M. V., and McKay, R. D., 2000. Transplanted CNS stem cells form functional synapses in vivo. Eur J Neurosci 12**,** 1696-1704.

3. Behrstock, S., and Svendsen, C. N., 2004. Combining growth factors, stem cells, and gene therapy for the aging brain. Ann N Y Acad Sci 1019**,** 5-14.

4. Benninger, F., Beck, H., Wernig, M., Tucker, K. L., Brustle, O., and Scheffler, B., 2003. Functional integration of embryonic stem cell-derived neurons in hippocampal slice cultures. J Neurosci 23**,** 7075-7083.

5. Collin, C., Vicario-Abejon, C., Rubio, M. E., Wenthold, R. J., McKay, R. D., and Segal, M., 2001. Neurotrophins act at presynaptic terminals to activate synapses among cultured hippocampal neurons. Eur J Neurosci 13**,** 1273-1282.

6. Conti, L., Cattaneo, E., and Papadimou, E., 2008. Novel neural stem cell systems. Expert Opin Biol Ther 8**,** 153-160.

7. Cooke, S. F., and Bliss, T. V. P., 2006. Plasticity in the human central nervous system. Brain 129**,** 1659-1673.

8. Copi, A., Jungling, K., and Gottmann, K., 2005. Activity- and BDNF-induced plasticity of miniature synaptic currents in ES cell-derived neurons integrated in a neocortical network. J Neurophysiol 94**,** 4538-4543.

9. Englund, U., Björklund, A., Wictorin, K., Lindvall, O., and Kokaia, M., 2002. Grafted neural stem cells develop into functional pyramidal neurons and

integrate into host cortical circuitry. Proc Natl Acad Sci USA 99**,** 17089-17094.

10. Englund, U., Ericson, C., Rosenblad, C., Mandel, R. J., Trono, D., Wictorin, K., and Lundberg, C., 2000. The use of a recombinant lentiviral vector for ex vivo gene transfer into the rat CNS. Neuroreport 11**,** 3973-3977.
11. Gage, F. H., 2000. Mammalian neural stem cells. Science 287**,** 1433-1438.
12. Glaser, T., Perez-Bouza, A., Klein, K., and Brustle, O., 2005. Generation of purified oligodendrocyte progenitors from embryonic stem cells. FASEB J 19**,** 112-114.
13. Glass, M., and Dragunow, M., 1995. Neurochemical and morphological changes associated with human epilepsy. Brain Res Brain Res Rev 21**,** 29-41.
14. Gottlieb, D. I., 2002. Large-scale sources of neural stem cells. Annu Rev Neurosci 25**,** 381-407.
15. Harris, E. W., and Cotman, C. W., 1986. Long-term potentiation of guinea pig mossy fiber responses is not blocked by N-methyl D-aspartate antagonists. Neurosci Lett 70**,** 132-137.
16. Jakubs, K., Nanobashvili, A., Bonde, S., Ekdahl, C. T., Kokaia, Z., Kokaia, M., and Lindvall, O., 2006. Environment Matters: Synaptic Properties of Neurons Born in the Epileptic Adult Brain Develop to Reduce Excitability. Neuron 52**,** 1047-1059.
17. Kanter-Schlifke, I., Toft Sørensen, A., Ledri, M., Kuteeva, E., Hökfelt, T., and Kokaia, M., 2007. Galanin gene transfer curtails generalized seizures in kindled rats without altering hippocampal synaptic plasticity. Neuroscience 150**,** 984-992.

18. Kim, S. U., and de Vellis, J., 2009. Stem cell-based cell therapy in neurological diseases: a review. J Neurosci Res 87**,** 2183-2200.

19. Kirschstein, T., von der Brelie, C., Steinhauser, M., Vincon, A., Beck, H., and Dietrich, D., 2004. L-CCG-I activates group III metabotropic glutamate receptors in the hippocampal CA3 region. Neuropharmacol 47**,** 157-162.

20. Kish, S. J., Shannak, K., and Hornykiewicz, O., 1988. Uneven pattern of dopamine loss in the striatum of patients with idiopathic Parkinson's disease. Pathophysiologic and clinical implications. N Engl J Med 318, 876-880.

21. Lepski, G., Jannes, C. E., Wessolleck, J., Kobayashi, E., and Nikkhah, G., 2010. Equivalent Neurogenic Potential of Wild-Type and GFP-Labeled Fetal-Derived Neural Progenitor Cells Before and After Transplantation Into the Rodent Hippocampus. Transplantation. Doi:10.1097/TP.0b013e3182063083

22. Li, T., Steinbeck, J. A., Lusardi, T., Koch, P., Lan, J. Q., Wilz, A., Segschneider, M., Simon, R. P., Brustle, O., and Boison, D., 2007. Suppression of kindling epileptogenesis by adenosine releasing stem cell-derived brain implants. Brain 130**,** 1276-1288.

23. Lindvall, O., and Kokaia, Z., 2006. Stem cells for the treatment of neurological disorders. Nature 441**,** 1094-1096.

24. Lindvall, O., and Kokaia, Z., 2010. Stem cells in human neurodegenerative disorders--time for clinical translation? J Clin Invest 120**,** 29-40.

25. Lundberg, C., Englund, U., Trono, D., Björklund, A., and Wictorin, K., 2002. Differentiation of the RN33B Cell Line into Forebrain Projection Neurons after Transplantation into the Neonatal Rat Brain. Exp Neurol 175**,** 370-387.

26. Lundberg, C., Winkler, C., Whittemore, S. R., and Björklund, A., 1996. Conditionally Immortalized Neural Progenitor Cells Grafted to the Striatum

Exhibit Site-Specific Neuronal Differentiation and Establish Connections with the Host Globus Pallidus. Neurobiol Dis 3**,** 33-50.

27. Lynch, M. A., 2004. Long-term potentiation and memory. Physiol Rev 84**,** 87-136.

28. Maciaczyk, J., Singec, I., Maciaczyk, D., Klein, A., and Nikkhah, G., 2009. Restricted spontaneous in vitro differentiation and region-specific migration of long-term expanded fetal human neural precursor cells after transplantation into the adult rat brain. Stem Cells Dev 18**,** 1043-1058.

29. Madhavan, L., Daley, B. F., Paumier, K. L., and Collier, T. J., 2009. Transplantation of subventricular zone neural precursors induces an endogenous precursor cell response in a rat model of Parkinson's disease. J Comp Neurol 515**,** 102-115.

30. Martinez-Serrano, A., and Bjorklund, A., 1997. Immortalized neural progenitor cells for CNS gene transfer and repair. Trends Neurosci 20**,** 530-538.

31. McBride, J. L., Behrstock, S. P., Chen, E. Y., Jakel, R. J., Siegel, I., Svendsen, C. N., and Kordower, J. H., 2004. Human neural stem cell transplants improve motor function in a rat model of Huntington's disease. J Comp Neurol 475**,** 211-219.

32. Miller, R. H., 2006. The promise of stem cells for neural repair. Brain Res 1091**,** 258-264.

33. Onifer, S. M., Whittemore, S. R., and Holets, V. R., 1993. Variable Morphological Differentiation of a Raphé-Derived Neuronal Cell Line Following Transplantation into the Adult Rat CNS. Exp Neurol 122**,** 130-142.

34. Paxinos, G., and Watson, C., 1996. The Rat Brain in Stereotaxic Coordinates.

35. Rosenqvist, N., Hård af Segerstad, C., Samuelsson, C., Johansen, J., and Lundberg, C., 2002. Activation of silenced transgene expression in neural precursor cell lines by inhibitors of histone deacetylation. J Gene Med 4**,** 248-257.

36. Rosser, A. E., Zietlow, R., and Dunnett, S. B., 2007. Stem cell transplantation for neurodegenerative diseases. Curr Opin Neurol 20**,** 688-692.

37. Ruschenschmidt, C., Koch, P. G., Brustle, O., and Beck, H., 2005. Functional properties of ES cell-derived neurons engrafted into the hippocampus of adult normal and chronically epileptic rats. Epilepsia 46 Suppl 5**,** 174-183.

38. Rutherford, L. C., Nelson, S. B., and Turrigiano, G. G., 1998. BDNF has opposite effects on the quantal amplitude of pyramidal neuron and interneuron excitatory synapses. Neuron 21**,** 521-530.

39. Shetty, A. K., and Hattiangady, B., 2007. Concise review: prospects of stem cell therapy for temporal lobe epilepsy. Stem Cells 25**,** 2396-2407.

40. Shetty, A. K., Rao, M. S., and Hattiangady, B., 2008. Behavior of hippocampal stem/progenitor cells following grafting into the injured aged hippocampus. J Neurosci Res 86**,** 3062-3074.

41. Shihabuddin, L. S., Hertz, J. A., Holets, V. R., and Whittemore, S. R., 1995. The adult CNS retains the potential to direct region-specific differentiation of a transplanted neuronal precursor cell line. J Neurosci 15**,** 6666-6678.

42. Shihabuddin, L. S., Holets, V. R., and Whittemore, S. R., 1996. Selective hippocampal lesions differentially affect the phenotypic fate of transplanted neuronal precursor cells. Exp Neurol 139**,** 61-72.

43. Turrigiano, G. G., 1999. Homeostatic plasticity in neuronal networks: the more things change, the more they stay the same. Trends Neurosci 22**,** 221-227.

44. Turrigiano, G. G., 2007. Homeostatic signaling: the positive side of negative feedback. Curr Opin Neurobiol 17**,** 318-324.

45. Vicario-Abejon, C., Collin, C., McKay, R. D., and Segal, M., 1998. Neurotrophins induce formation of functional excitatory and inhibitory synapses between cultured hippocampal neurons. J Neurosci 18**,** 7256-7271.

46. Wernig, M., Benninger, F., Schmandt, T., Rade, M., Tucker, K. L., Bussow, H., Beck, H., and Brustle, O., 2004. Functional integration of embryonic stem cell-derived neurons in vivo. J Neurosci 24**,** 5258-5268.

47. Whitehouse, P. J., Price, D. L., Clark, A. W., Coyle, J. T., and DeLong, M. R., 1981. Alzheimer disease: evidence for selective loss of cholinergic neurons in the nucleus basalis. Ann Neurol 10**,** 122-126.

48. Whittemore, S. R., and White, L. A., 1993. Target regulation of neuronal differentiation in a temperature-sensitive cell line derived from medullary raphe. Brain Res 615**,** 27-40.

49. Wierenga, C. J., Ibata, K., and Turrigiano, G. G., 2005. Postsynaptic expression of homeostatic plasticity at neocortical synapses. J Neurosci 25**,** 2895-2905.

50. Zalutsky, R. A., and Nicoll, R. A., 1990. Comparison of two forms of long-term potentiation in single hippocampal neurons. Science 248**,** 1619-1624.

TABLE LEGENDS

Table 1: Intrinsic membrane properties of transplanted and fully differentiated GFP-positive cells and endogenous host pyramidal cells in CA3 of the hippocampus. □p < 0.01, Student *t*-test.

FIGURE LEGENDS

Fig 1. Transplanted GFP-labeled neuronal progenitor cells turn into fully differentiated projection neurons. Typical morphology and appearance of GFP-labeled cells at 2 (A), 7 (B), 21 (C) and 28 (D) days following transplantation. (A) On the second day, round shaped GFP-positive cells are mostly confined to cluster of cells, (B) before gradually spreading and migrate away from the graft site. Around 21 days following transplantation, dendritic processes are detected in connection and close vicinity of GFP-positive cell somas (C), when the cells begin to appear in the principal cell layer of the hippocampus. (D) Twenty-eight days following transplantation, cells bodies of fully differentiated GFP-positive cells (marked by arrows) found preferentially within the principal cell layer of CA3. Red layers highlight the principal cell layers of the slice, whereas single red dots in fiber layers depict single interneurons. Neuronal nuclei staining, NeuN, visualizes in red color neuronal cell bodies. Boxed area on left is magnified on right. (E) Illustration of hippocampal slices showing transplantation site and typical route of migration of GFP-positive cells from *A* towards *B,* before incorporation into the principal cell layer in *C*, *F* area. Placement of letters applies to orientation of A, B, C and F images. (F) Fully differentiated and mature GFP-positive cell 56 days following transplantation incorporated into stratum pyramidale of CA3. Scale bars in A-F = 100 μm.

Fig 2. Intrinsic membrane properties of GFP-positive and principal cells in CA3 area. Typical patterns of membrane rectification in host pyramidal (A) and GFP-positive (B) cell recorded in CA3 stratum pyramidal. Higher action potential threshold can be noted in the GFP-positive cell, in which additional positive current steps applied via patch pipette are needed before reaching the action potential threshold. Magnification

of action potential in host pyramidal (C) and GFP-positive (D) cell. Positions for measuring action potential threshold, amplitude and duration are shown by arrows. (E and F) Average *I-V* relationships of all recorded cells in CA3 stratum pyramidal. No differences were detected between host pyramidal (E) (n = 6) and GFP-positive (F) (n = 7) cells. During whole-cell patch-clamp recordings of transplanted GFP-positive (G) and endogenous principal cells (H) passive diffusion of biocytin marked the dendrites of the cells. All GFP-positive cells were retrospectively confirmed to be double-labeled, as indicated by yellow color of merged images of biocytin and GFP signaling. Scale bar = 150 μm (applies for all images).

Fig 3. Functional synapse formation on transplanted GFP-positive cells in CA3. (A) Representative traces of sEPSC recorded in GFP-positive and endogenous host pyramidal cells in CA3. Off-line analysis using Kolmogorov-Smirnov test revealing significant shorter interevent intervals (IEI) (B) and higher amplitudes (C) of sEPSCs in GFP-positive cells (n = 5) as compared to host pyramidal cells (n = 5) in CA3. The paired-pulse (PP) ratio of evoked EPSCs is equal for GFP-positive and pyramidal cells in CA3. During aCSF application (D) paired-pulse depression (PPD) is recorded in GFP-positive (n = 14) and host pyramidal (n = 9) cells, while blocking $GABA_A$ receptors by additional PTX application (E) turns PPD into paired-pulse facilitation (PPF) in GFP-positive (n = 14) and host pyramidal (n = 6) cells. (F) Dendritic spines as seen in CA3 stratum radiatum (marked by arrows) belonging to a recorded GFP-positive cell in CA3, visualized by GFP (green), biocytin (red) and merged colors (yellow). (G) Dendritic spines of a biocytin-filled host pyramidal cell in CA3 visualized in the same subfield as in *F*. Scale bar in F, G = 5 μm.

Fig 4. LTP expression in transplanted GFP-positive cells. (A) High-frequency stimulation (HFS) of A/C fibers inducing stable and long-lasting synaptic potentiation (LTP) of evoked EPSCs in GFP-positive cells (n = 3) situated in CA3. Synaptic potentiation continues for at least 30 min, and its magnitude, expressed as normalized EPSC amplitudes (average of four EPSCs per min), is comparable to the level recorded in endogenous CA3 pyramidal cells (n = 4). Inserts showing representative traces of evoked EPSCs recorded 1 min before (1) and 20 min after (2) HFS in transplanted GFP-positive and host CA3 pyramidal cell, respectively. Scale bar applies for all traces. (B) Post-tetanic potentiation (PTP) normalized to average baseline values and determined each min during 5 min following HFS for GFP-positive (n = 9) and host CA3 pyramidal (n = 12) cells.

TABLE 1

	CA3	
	GFP-positive (n = 7)	Host (n = 6)
Resting membrane potential (mV)	-70.1 ± 0.7	-68.3 ± 0.8
Input resistance (MΩ)	162 ± 19	203 ± 10
Action potential threshold (mV)	-36.7 ± 1.7	-45.2 ± 1.4
Action potential amplitude (mV)	91.9 ± 5.9	85.4 ± 4.0
Action potential duration (ms)	1.6 ± 0.1	1.7 ± 0.1

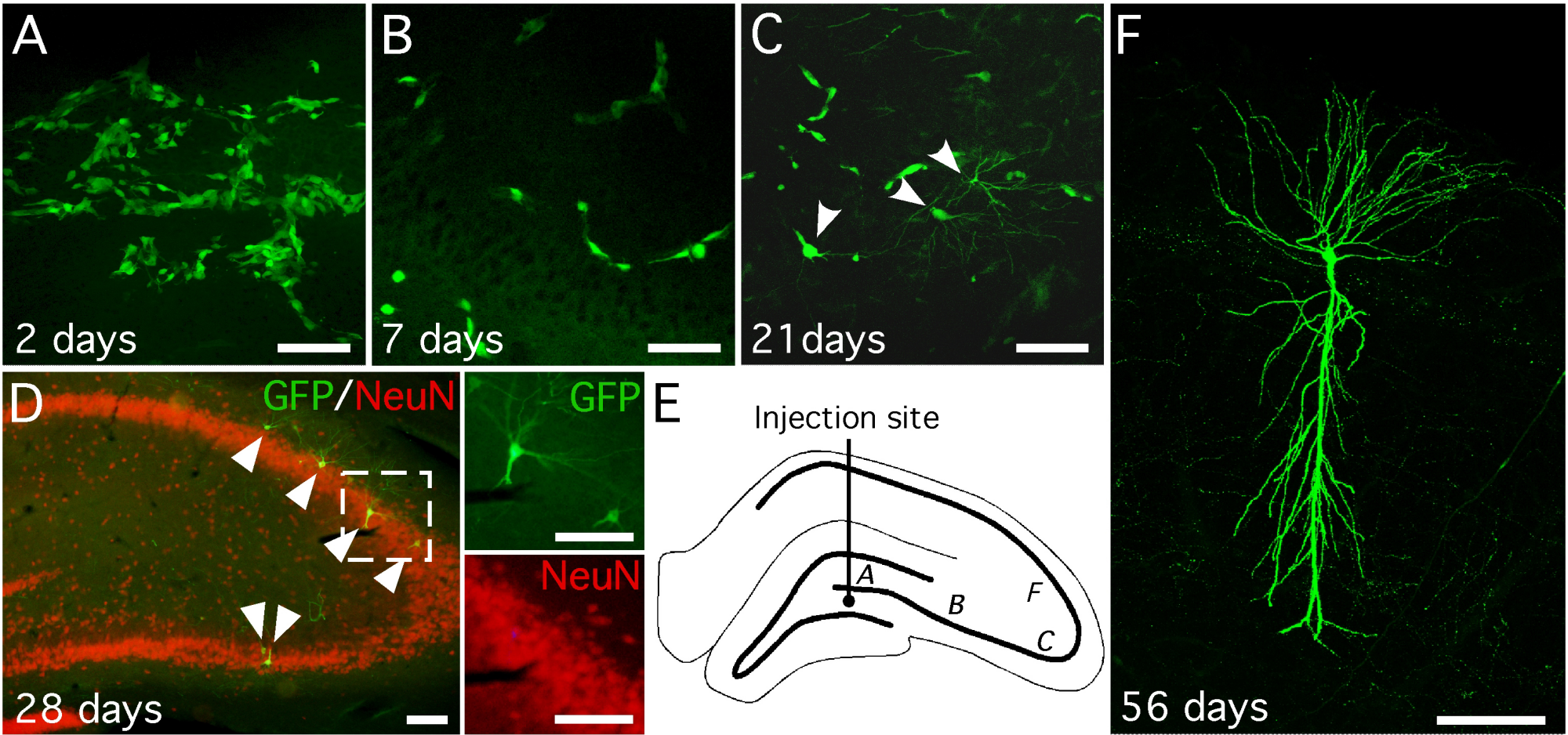
A
2 days
B
7 days
C
21days
F
56 days
D
GFP/NeuN
28 days
GFP
NeuN
E
Injection site
A
B
C
F

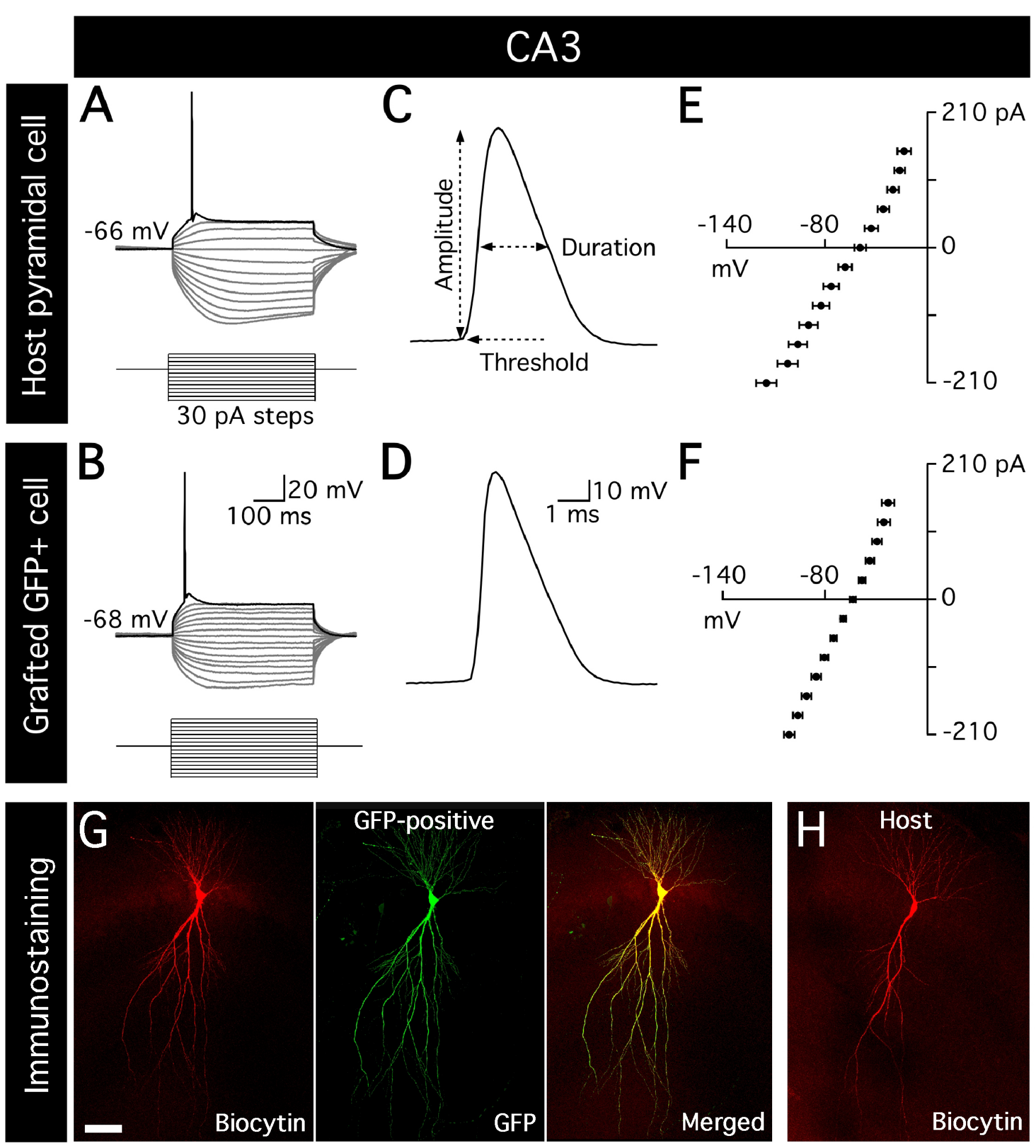
CA3
Host pyramidal cell
A
-66 mV
30 pA steps
C
Amplitude
Duration
Threshold
E
210 pA
-140
-80
0
mV
-210
Grafted GFP+ cell
B
20 mV
100 ms
-68 mV
D
10 mV
1 ms
F
210 pA
-140
-80
0
mV
-210
Immunostaining
G
Biocytin
GFP-positive
GFP
Merged
H
Host
Biocytin

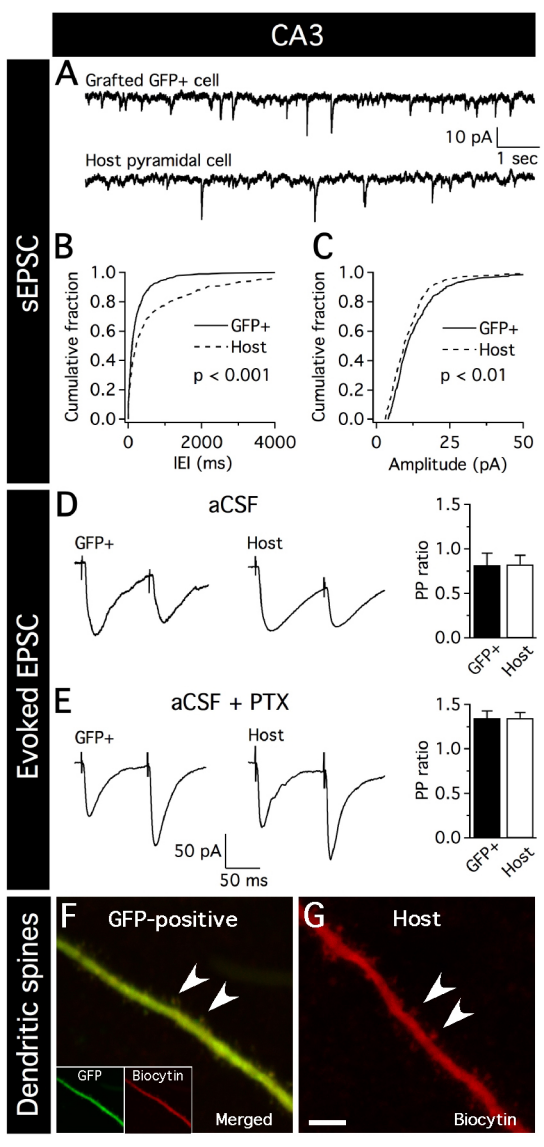
CA3
sEPSC
A
Grafted GFP+ cell
10 pA
1 sec
Host pyramidal cell
B
Cumulative fraction
GFP+
Host
p < 0.001
IEI (ms)
C
Cumulative fraction
GFP+
Host
p < 0.01
Amplitude (pA)
Evoked EPSC
D
aCSF
GFP+
Host
PP ratio
E
aCSF + PTX
GFP+
Host
50 pA
50 ms
PP ratio
Dendritic spines
F
GFP-positive
GFP
Biocytin
Merged
G
Host
Biocytin

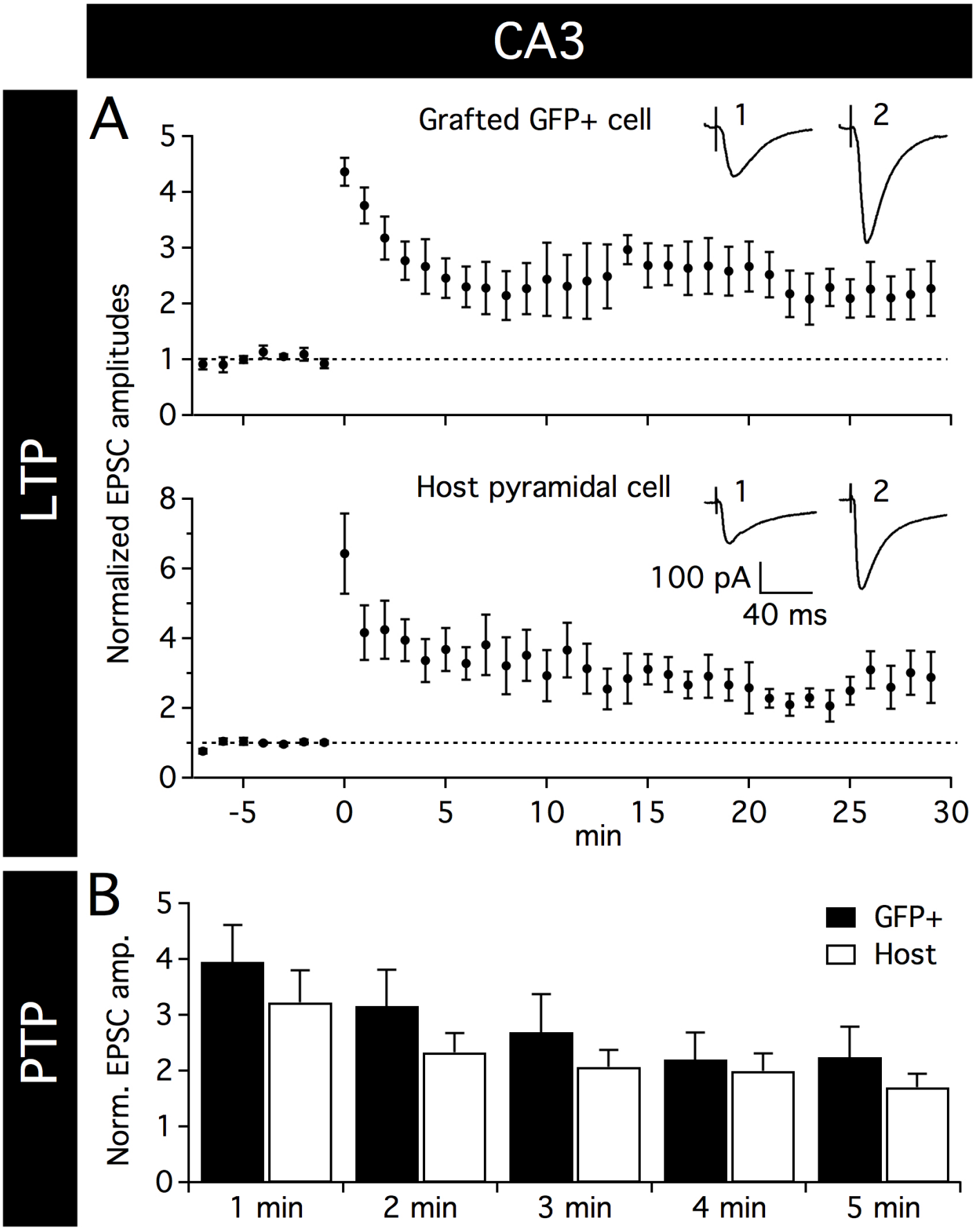
CA3
LTP
A
Grafted GFP+ cell
1
2
Normalized EPSC amplitudes
Host pyramidal cell
100 pA
40 ms
min
PTP
B
Norm. EPSC amp.
GFP+
Host
1 min
2 min
3 min
4 min
5 min

SUPPLEMENTARY DATA

Supplementary text

In two GFP-positive cells recorded in CA1 (56.5 ± 0.7 days post grafting) and one GFP-positive cell recorded in DG (47 days post grafting), the intrinsic membrane properties including membrane rectification upon hyperpolarization/depolarization steps appeared similar to endogenous CA1 (52.3 ± 2.3 days old, n = 6) and granule cells (46.9 ± 2.4 days old, n = 7) (Suppl. Figs. 1A, B, C and D), respectively. Due to limited number of recordings of GFP-positive cells in these areas, statistical comparison to similar positioned endogenous principal cells was unattainable. Nonetheless, recorded GFP-positive and endogenous pyramidal cells in CA1 had resting membrane potential of -72.5 ± 3.5 mV and -66.8 ± 0.8 mV, respectively, whereas the input resistance was 385 ± 84 MΩ and 253 ± 20 MΩ, respectively. The action potential properties of GFP-positive cells (and endogenous pyramidal cells) in CA1 was; threshold (mV): -39.6 ± 10.0 (-52.0 ± 1.3), amplitude (mV): 92.4 ± 8.0 (99.0 ± 4.3) and duration (ms): 1.6 ± 0.2 (1.6 ± 0.1). For GFP-positive cell in DG (and endogenous granule cells); resting membrane potential (mV): -80 (-82.1 ± 0.8), input resistance (MΩ): 442 (431 ± 61), threshold (mV): -54.8 (-41.5 ± 2.3), amplitude (mV): 108.4 (84.6 ± 4.1) and duration (ms): 1.7 (1.6 ± 0.1).

In two other GFP-positive cells with cell body in CA1 stratum pyramidale, paired-pulse stimulations delivered to stratum radiatum in CA1 evoked monosynaptic EPSCs displaying PPD with average ratio of 0.61 ± 0.16 during aCSF application (Suppl. 1A). Recordings of endogenous CA1 pyramidal cells confirmed that PPD (0.93 ± 0.11, n = 7 cells, Suppl. 1B) of evoked EPSCs is not unusual in Schaffer collateral-CA1 synapses when $GABA_A$ receptors are not blocked by PTX. In addition,

paired stimulation of the MPP evoked monosynaptic EPSCs showing PPD (average ratio of 0.84) in two GFP-positive cells situated in stratum granulosum of the dentate gyrus (Suppl. 1C), whereas control recordings of host dentate granule cells revealed PPD ratio of 0.73 ± 0.04 (n = 9 cells) in MPP synapses (Suppl. 1D).

Supplementary Fig. 1 Supplementary text

Supplementary Fig 1 Functional properties of GFP-positive cells in CA1 and DG area. Stepwise current pulses of 30 pA increments evoking action potential in fully differentiated GFP-positive cells in CA1 (A) and DG (C) region. Note, that both resting membrane potential and rectification patterns closely resemble endogenous principal cells recorded in similar regions (B and D). Paired-pulse stimulation of Schaffer collateral fibers and medial perforant path (MPP) inducing evoked EPSCs in CA1 and DG, respectively, in GFP-positive (A and C) and endogenous host cells (B and D). The rate of PPD appears similar in GFP-positive and endogenous host cells. Both transplanted GFP-positive and endogenous host principal cell were marked by biocytin during recordings, and GFP-positive cells were retrospectively confirmed to be double-labeled, as indicated by yellow color of merged images of biocytin (red) and GFP (green) signaling. Scale bar in CA1 = 150 μm (*A* and *B*), DG = 50 μm (*C* and *D*).

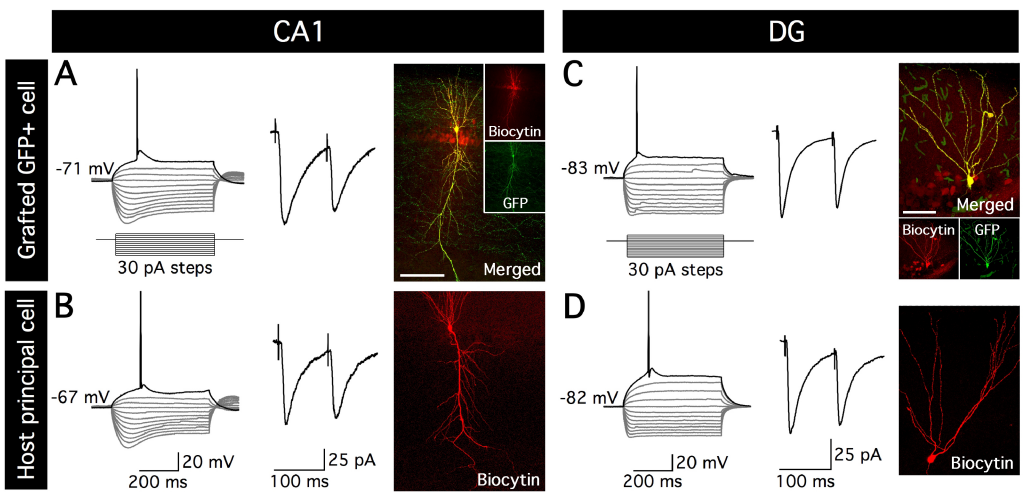
CA1
DG
Grafted GFP+ cell
Host principal cell
A
B
C
D
-71 mV
30 pA steps
Biocytin
GFP
Merged
-67 mV
20 mV
200 ms
25 pA
100 ms
Biocytin
-83 mV
30 pA steps
Merged
Biocytin
GFP
-82 mV
20 mV
200 ms
25 pA
100 ms
Biocytin